Virology 482 (2015) 244–259

Contents lists available at ScienceDirect

Virology

journal homepage: www.elsevier.com/locate/yviro

Acetylation of intragenic histones on HPV16 correlates with enhanced HPV16 gene expression

Cecilia Johansson, Tavan Jamal Fattah, Haoran Yu, Jakob Nygren, Ann-Kristin Mossberg, Stefan Schwartz *

Department of Laboratory Medicine, Lund University, 221 84 Lund, Sweden

ARTICLE INFO

Article history:
Received 10 December 2014
Returned to author for revisions
23 January 2015
Accepted 25 February 2015
Available online 17 April 2015

Keywords:
HPV16
Papillomavirus
Epigenetics
Histone marks
H3K9Ac
H3K36me3
H3K9me3
H4K20me3
H2BK5me1
HDAC inhibitor
Splicing
Polyadenylation
SR proteins
Hnrnp
Panobinostat
Quisinostat

ABSTRACT

We report that many histone modifications are unevenly distributed over the HPV16 genome in cervical cancer cells as well as in HPV16-immortalized keratinocytes. For example, H3K36me3 and H3K9Ac that are common in highly expressed cellular genes and over exons, were more common in the early than in the late region of the HPV16 genome. In contrast, H3K9me3, H4K20me3, H2BK5me1 and H4K16Ac were more frequent in the HPV16 late region. Furthermore, a region encompassing the HPV16 early polyadenylation signal pAE displayed high levels of histone H3 acetylation. Histone deacetylase (HDAC) inhibitors caused a 2- to 8-fold induction of HPV16 early and late mRNAs in cervical cancer cells and in immortalized keratinocytes, while at the same time increasing the levels of acetylated histones in the cells and on the HPV16 genome specifically. We concluded that increased histone acetylation on the HPV16 genome correlates with increased HPV16 gene expression.

Introduction

Human papillomavirus (HPV) is the most common sexually transmitted virus in the human population. It is present in 99.7% of all cervical cancers and is tightly associated with other anogenital cancers as well as head and neck cancers (Walboomers et al., 1999). More than 500,000 cases of cervical cancers are diagnosed each year in the world and cervical cancer is one of the main causes of death of women in the developing world (Walboomers et al., 1999). Although the vast majority of the genital HPV infections are cleared by the immune system within a year after infection, and as such pose little threat to the health of the infected individual, HPVs may in rare cases persist and cause cancer (zur Hausen, 2002). These persistent HPV infections are generally caused by a subset of the sexually transmitted HPVs termed high-risk HPV types. HPV type 16 is the most common high-risk type in cervical cancers as well as in the human population (Bouvard et al., 2009; Bosch et al., 2002). How HPV16 can persist in the presence of a functional immune system is an enigma but is likely a result of the ability of HPV16 to interfere with the immune system of the host, and its ability to restrict expression of the highly immunogenic L1 and L2 capsid proteins to a late stage in the viral life cycle, at the very top of the infected mucosal epithelium (Chow et al., 2010; Bodily and Laimins 2011; Doorbar, 2005). Controlling HPV16 gene expression is therefore of paramount importance for establishment of persistence (Johansson and Schwartz, 2013).

The HPV16 DNA genome can be divided into an early and a late region (Fig. 1A) (Howley and Lowy, 2006). The early region is coding for E1, E2, E4, E5, E6 and E7 and is followed by the early polyA signal pAE, while the late region encodes L1 and L2 and is

* Correspondence to: Department of Laboratory Medicine, Lund University, BMC-B13, room B1314c, 223 62 Lund, Sweden. Tel.: +46 46 2220628/ 46 46 222062829, Mobile: +4673 9806233.
E-mail address: Stefan.Schwartz@med.lu.se (S. Schwartz).

http://dx.doi.org/10.1016/j.virol.2015.02.053
0042-6822/

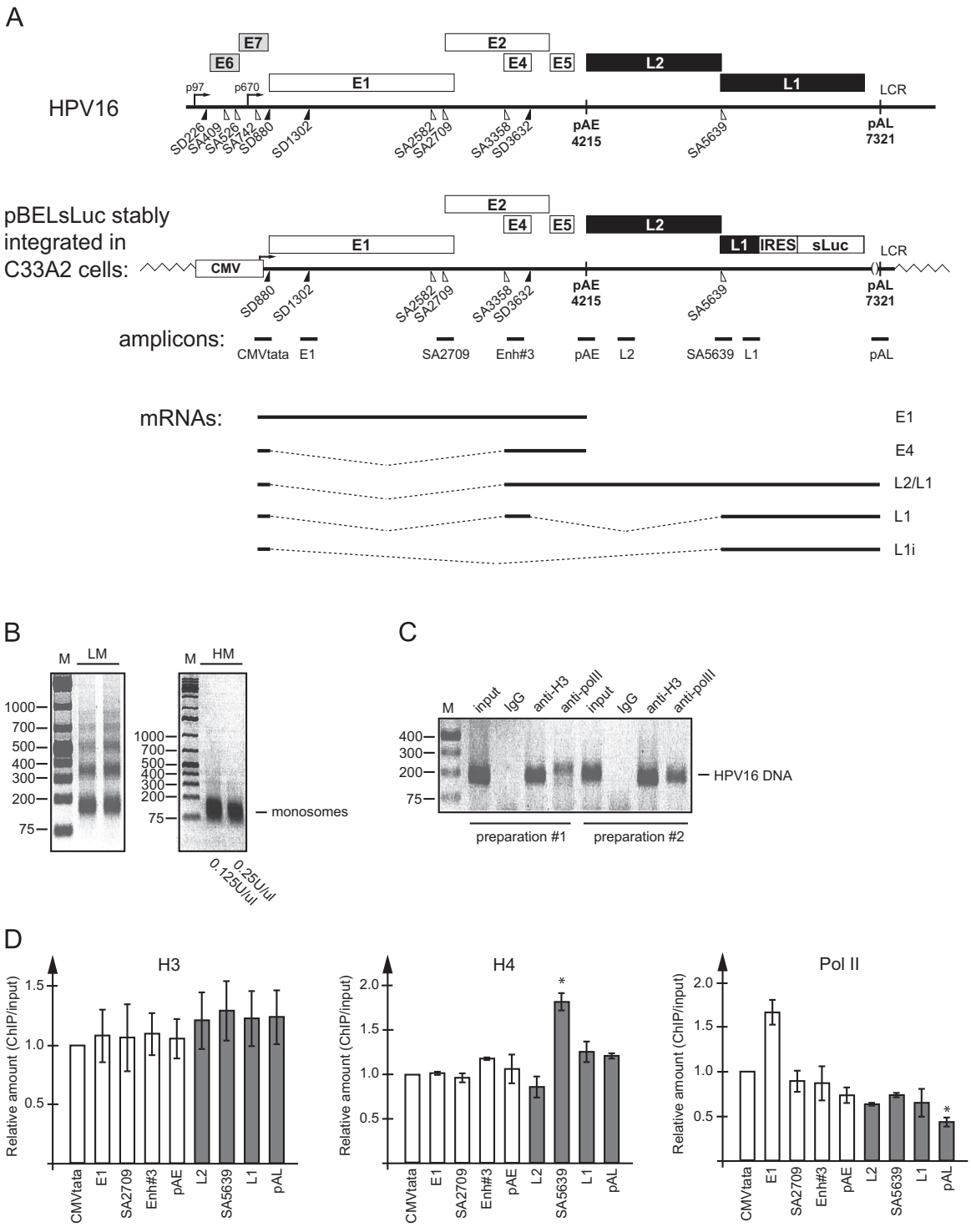

Fig. 1. (A) Schematic representation of the HPV16 genome depicting open reading frames as rectangles, the early and late promoters p97 and p670 respectively, as arrows and splice sites as triangles. The long control region (LCR) and the early and late polyA signals pAE and pAL are indicated. Schematic drawing of the HPV16 pBELsLuc reporter plasmid integrated in the cellular genome of the C33A-derived reporter cell line C33A2 (Li et al., 2013). A subset of early and late mRNAs that may be produced from the pBELsLuc is indicated. The locations of amplicons produced in ChIP assays with primers listed in Table S1 are indicated. (B) DNA extracted from MNase treated chromatin prepared from C33A2 cells were separated on agarose gels and stained with GelRed nucleic acid staining. LM and HM indicated low and high levels of MNase, respectively. The higher levels yielded primarily monosomes and were used for all preparations. (C) PCR of HPV16 DNA with primers L2F and L2R (L2 amplicon) on chromatin immunoprecipitations performed with IgG, anti-histone H3- or anti-RNA polymerase-II-antibodies on two independently prepared nucleosome preparations. PCR with the same primers was also performed on each nucleosome preparation that was used for ChIP (input). (D–F) ChIP analyses on C33A2 cells using antibodies to proteins indicated in each histogram and qPCR of the indicated amplicons. Primers and antibodies are listed in Tables S1 and S2 respectively. Mean values with standard deviations of the amount of immunoprecipitated DNA compared to input DNA are displayed. For antibodies to H3, H4 and RNA polymerase II, the values for the CMVtata PCR was set to 1 to correct for differences between different ChIP extracts. White bars represent HPV16 early genes and gray bars represent late genes. *p*-Values were calculated for each ChIP result in relation to the CMVtata amplicon (D) or the E1 amplicon (E, F and H). *p*-Values less than 0.05 (*) or 0.01 (**) are indicated. All samples were analyzed in two independent ChIP assays and all qPCR reactions were performed in triplicates. (G) Secreted luciferase activity in the cell culture medium of C33A2 cells incubated with 5 μM of the indicated demethylase inhibitors for 24 h. DMSO was used as a negative control and TPA as a positive control. Graph shows mean values and standard deviations of fold induction of sLuc activity of each drug compared to DMSO. Results are from three independent experiments performed in triplicates. *p*-Values were calculated with sLuc results from each drug compared to sLuc results from C33A2 cells incubated with DMSO. All sLuc measurements were obtained from at least three independent cell treatments and were analyzed in triplicates. *p*-Values less than 0.05 (*) or 0.01 (**) are indicated. (H) Chromosomal DNA prepared from C33A2 cells subjected to methyl-cytosine DNA immunoprecipitation followed by qPCR of the indicated amplicons. *p*-Values were calculated for each primer pair in relation to the E1 amplicon. *p*-Values less than 0.05 (*) or 0.01 (**) are indicated. All samples were analyzed in two independent assays and all qPCR reactions were performed in triplicates. (I) sLuc activity in the cell culture medium of C33A2 cells incubated with 5 μM of the indicated DNA methyltransferase inhibitors azacitidine or RG108. *p*-Values were calculated with sLuc results from each drug compared to sLuc results from C33A2 cells incubated with DMSO. All sLuc measurements were obtained from at least three independent cell treatments and were analyzed in triplicates. None of the *p*-values were less than 0.05.

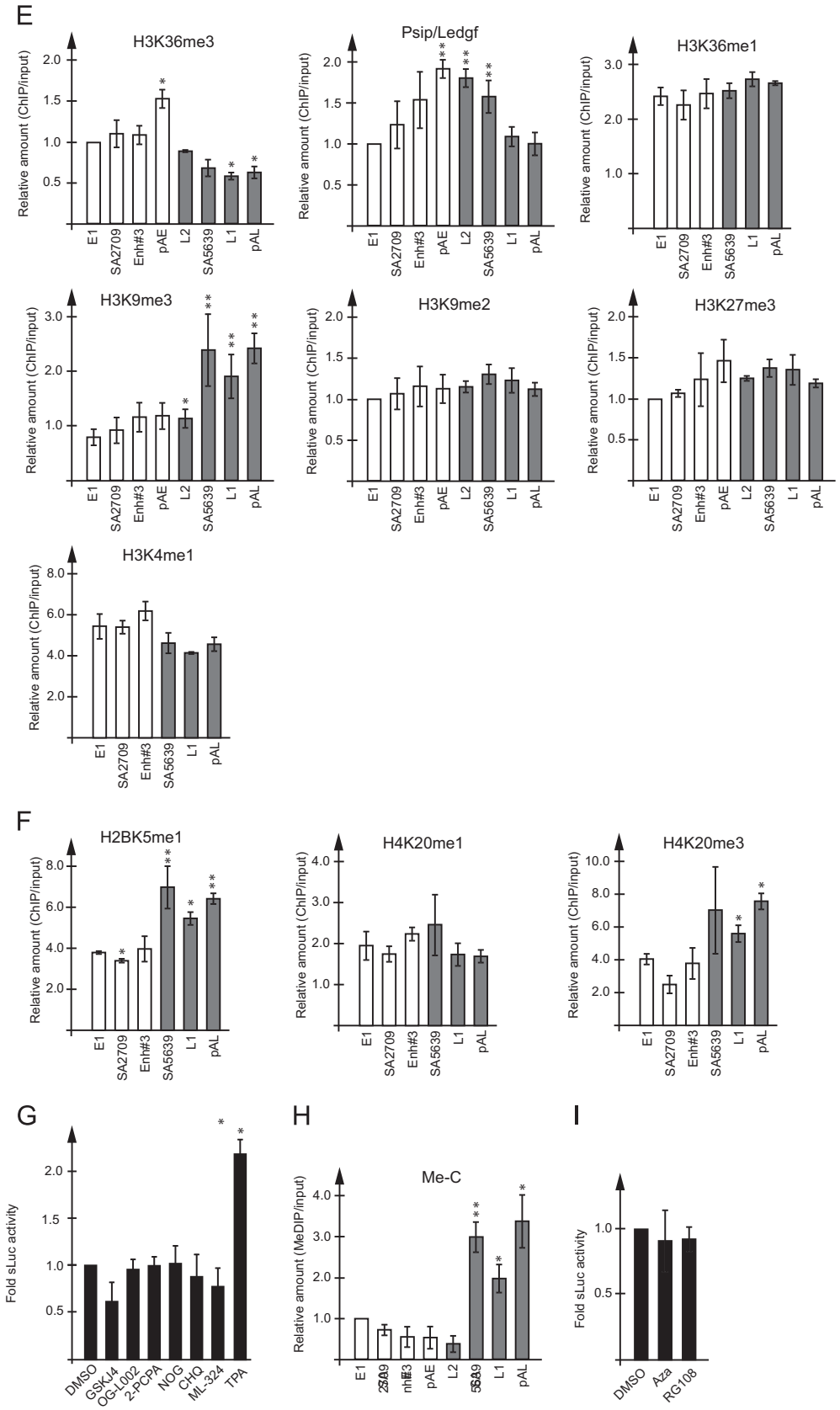

Fig. 1. (*continued*)

followed by the late polyA signal pAL. The early promoter p97 is situated upstream of the E6 gene and could potentially produce mRNAs encoding all HPV proteins, while the late promoter p670 is situated upstream of the E1 gene and therefore cannot be used to express the E6 and E7 genes (Schwartz, 2013; Baker and Calef, 1997). HPV16 gene expression is controlled at the level of

transcription (Bernard, 2013), which is regulated by both HPV16 E2 and by cellular factors (McBride, 2013; Thierry, 2009). HPV16 gene expression is also regulated at the level of polyadenylation which includes a switch from the early polyA signal (pAE) to the late polyA signal (pAL), and at the level of splicing as evidenced by the high number of alternatively spliced mRNAs that produced during the viral life cycle (Johansson and Schwartz, 2013; Schwartz, 2013; Graham, 2008; Jia and Zheng, 2009).

The efficiency by which a splice site is used is determined by cis-acting regulatory RNA elements termed splicing enhancers and silencers (Cartegni et al., 2002). Many of the HPV16 splice sites are controlled by cis acting RNA elements (Johansson and Schwartz, 2013). For example, the efficiently used 3′-splice site SA3358 used by both early and late HPV16 mRNAs is dependent on a strong splicing enhancer located downstream of SA3358 (Rush et al., 2005; Somberg and Schwartz, 2010; Li et al., 2013). This enhancer interacts with ASF/SF2 (SRSF1), SRp30c (SRSF9) and SRp20 (SRSF3) (Somberg and Schwartz, 2010; Li et al., 2013; Somberg et al., 2011; Jia et al., 2009, 2010). Lack of splicing to SA3358 reduces polyadenylation at pAE, demonstrating that the splicing enhancer downstream of SA3358 is a key regulatory element in the HPV16 life cycle (Rush et al., 2005; Li et al., 2013). Furthermore, HPV16 late splice sites SD3632 and SA5639 that are used exclusively to produce the late L1 mRNAs, are under control of splicing silencers that interact with hnRNP A1 for SA5639 (Zhao et al., 2004, 2007; Zhao and Schwartz, 2008), and with hnRNP D-proteins and hnRNP A2/B1 for SD3632 (Li et al., 2013). On the other hand, hnRNP A1 enhances splicing of the HPV16 early mRNAs (Rosenberger et al., 2010). The HPV16 early polyA signal is also subject to regulation, and a reduction in polyadenylation efficiency is required for activation of HPV16 late gene expression (Zhao et al., 2005; Jeon and Lambert, 1995). The HPV16 E2 protein interferes with the polyadenylation complex at pAE thereby inducing HPV16 late gene expression (Johansson et al., 2012). The HPV16 early polyA signal is under positive control of the upstream, untranslated region (Zhao et al., 2005; Jeon and Lambert, 1995) and by downstream elements spanning the L2 coding region (Oberg et al., 2005). In contrast, the late polyA signal is strongly suppressed by sequences in the late UTR that are active at least in mitotic cells (Graham, 2008). Thus, RNA processing plays a major role in HPV16 gene regulation (Johansson and Schwartz, 2013).

Although it is well established that the state of the chromatin control transcription of cellular genes, recently published results indicate that chromatin and epigenetic properties of chromosomal DNA within genes such as nucleosome positioning, histone methylation, acetylation and phosphorylation may contribute to the control of RNA splicing and polyadenylation by recruiting RNA processing factors to DNA sequences encoding splicing regulatory RNA elements (Braunschweig et al., 2013; Brown et al., 2012; Acuna et al., 2013; Schwartz and Ast, 2010; Luco and Misteli, 2011; Iannone and Valcárcel, 2013). For example, H3K36me3 and H3K9me3 are enriched over exons and may recruit splicing factors (Barski et al., 2007; Wang et al., 2008; Luco et al., 2010; Pradeepa et al., 2012; Saint-Andre et al., 2011), while high levels of H3K9Ac are associated with exon skipping (Zhou et al., 2011; Schor et al., 2009). Posttranslational modifications of histones on the HPV16 genome could therefore potentially control HPV16 gene expression. It has also recently been shown that the HPV16 genome is subject to epigenetic modifications over the viral replication cycle, in particular DNA methylation although the significance of these modifications is unclear (Szalmás and Kónya, 2009; Steenbergen et al., 2014). Furthermore, chromatin immunoprecipitations performed on HeLa cell chromatin have indicated that histone marks on the HPV18 sequences in HeLa cells are unevenly distributed over the HPV18 genome, suggesting a role for histone modifications in the control of HPV18 gene expression (Johannsen and Lambert, 2013). The papillomavirus E2 proteins interact with chromatin and could potentially control gene expression by interfering with histone function (McBride et al., 2012). We therefore wished to investigate if epigenetic properties of the HPV16 genome could potentially control HPV16 gene expression.

Results

Low levels of H3K36me3 and high levels of H3K9me3, H4K20Me3 and H2BK5me1 in the HPV16 late genes in cervical cancer cells

In order to investigate if epigenetic properties of the HPV16 genome such as DNA methylation and histone modifications contribute to HPV16 gene regulation, we used the HPV16 reporter cell line C33A2 (Fig. 1A). This cell line contains the subgenomic HPV16 expression plasmid pBELsLuc stably integrated into its genome (Fig. 1A) (Li et al., 2013). It expresses high levels of early HPV16 mRNAs, in particular E4 mRNAs spliced between SD880 and SA3358 followed by polyadenylation at pAE, but only low levels of the late mRNAs (Zhao et al., 2004; Orru et al., 2012). pBELsLuc has the sLuc gene inserted into the L1 coding region of HPV16 and it serves as a marker for HPV16 late gene expression (Li et al., 2013). The HPV16 late mRNAs can be induced by overexpression or knock-down of various proteins and this induction can be monitored as an increase in secreted luciferase (sLuc) in the cell culture medium.

To investigate if histone marks on the HPV16 genome, correlated with the high levels of early gene expression or the low levels of late gene expression in the C33A2 cells, a screening of various histone marks over the integrated pBELsLuc plasmid in the C33A2 cells was performed using chromatin immunoprecipitation (ChIP) assay. First, the MNase digestion of the chromatin was optimized to produce mononucleosomes and dinucleosomes (Fig. 1B). that were subjected to ChIP assay with either IgG, or antibodies to histone H3 or RNA polymerase-II followed by PCR on the extracted DNA with HPV16 primers (Fig. 1C). These results revealed that HPV16 DNA could be immunoprecipitated with antibodies to histone H3 and RNA polymerase-II, but not by IgG (Fig. 1C). A PCR fragment of the same size was amplified from the input chromatin preparation, as expected (Fig. 1C). Having established appropriate ChIP conditions, the levels of nucleosomes immunoprecipitated by each antibody were determined by qPCR as described in section “Materials and methods”. First results revealed that the levels of total histone H3 and H4 were relatively similar over the entire HPV16 sequence (Fig. 1D), while levels of RNA polymerase II on the HPV16 genome decreased somewhat as the distance from the promoter grew (Fig. 1D). Next we investigated if histone methylation correlated with HPV16 gene expression levels. We found that the levels of H3K36me3 were lower in the late region than in the early region (Fig. 1E), which is in line with previous observations of enrichment of H3K36me3 on exons and transcribed regions of DNA (Barski et al., 2007; Wagner and Carpenter, 2012; Spies et al., 2009; Andersson et al., 2009). Splicing factors of the SR protein family have been shown to bind H3K36 in a Psip/Ledgf-dependent manner (Pradeepa et al., 2012). However, the levels of Psip/Ledgf p52 associated with HPV16 DNA were not higher in the early region than in the early region (Fig. 1E). Levels of mono-methylated H3K36 (H3K36me1) on the other hand were similar over HPV16 early and late genes (Fig. 1E). Presence of H3K9me3 has been shown to correlate with transcription repression (Barski et al., 2007; Wang et al., 2008) but is also enriched over alternatively spliced exons and interact with splicing factors (Saint-Andre et al., 2011). H3K9me3 displayed an inverse correlation with HPV16 gene expression and was more

abundant in the HPV16 late region than in the early region (Fig. 1E), while H3K9me2 was evenly distributed over the HPV16 genome (Fig. 1E). H3K27me3 that has previously been reported to be enriched over exons and to be associated with splicing factor HP1alpha (Spies et al., 2009; Andersson et al., 2009) was evenly distributed over the HPV16 genome (Fig. 1E), whereas H3K4me1 that has not previously been associated with splicing was slightly less abundant in the HPV16 late region (Fig. 1E). It has been reported that the histone H2B mark H2BK5me1 is enriched over exons (Barski et al., 2007; Andersson et al., 2009). However, here it was more abundant over the HPV16 late genes than the early genes (Fig. 1F). Analysis of methylation of histone H4 revealed that H4K20me1 was evenly distributed over HPV16 early and late genes, while H4K20me3 was more abundant over the late genes (Fig. 1F) and therefore showed an inverse correlation with HPV16 gene expression levels.

We wished to investigate if altering the levels of histone methylation affected HPV16 gene expression. Levels of H3K3-6me3 and H3K4me1 have been shown previously to be low in poorly expressed cellular genes (Barski et al., 2007; Wagner and Carpenter 2012; Spies et al., 2009; Andersson et al., 2009), which correlate well with the lower levels of H3K36me3 and H3K4me1 in the late region of HPV16. These results suggested that enhanced histone methylation might alleviate inhibition of HPV16 late gene expression. We therefore investigated if histone de-methylase inhibitors that would prevent de-methylation of H3K4me1 (OG-L002 and 2-PCPA), H3K36me3 (NOG, CHQ and ML234) or H3K27 (GSK J4 HCl) affected HPV16 late gene expression (Fig. 1G). However, none of the histone demethylase inhibitors induced HPV16 late gene expression whereas the positive control substance TPA that has been shown previously to induce HPV16 (Orru et al., 2012) or HPV31 (Meyers et al., 1992) late gene expression, induced late gene expression in the C33A2 cells, which was as measured as an increase in secreted luciferase activity in the cell culture medium of the C33A2 cells (Fig. 1G).

High levels of methylated DNA in the late region of HPV16

We also monitored the levels of HPV16 DNA methylation in the C33A2 cell line using methyl-DNA immunoprecipitation and found high levels of DNA methylation in the HPV16 late region compared to the early region (Fig. 1H), suggesting that methylation of HPV16 late DNA suppressed HPV16 late gene expression. However, treatment of the C33A2 cells with either reversible or non-reversible DNA methyltransferase inhibitors azacytidine and RG108 had no effect on HPV16 late gene expression (Fig. 1I). In contrast, the positive control substance TPA did as expected (Fig. 1G).

Low levels of histone H3 acetylation (H3K9Ac) in the HPV16 late genes but high levels at the early polyA signal

Next we investigated if histone-acetylation on HPV16 nucleosomes correlated with HPV16 gene expression levels. As can be seen from Fig. 2A, the levels of histone 3 acetylation, in particular H3K9Ac, was significantly lower in the HPV16 late region, than in the early region. In contrast, levels of histone H4 acetylation and H4K8Ac showed a peak at the promoter, but remained relatively constant over the HPV16 early and late genes (Fig. 2A). H4K16Ac was elevated at late 3′-splice site SA5639, but otherwise displayed a similar degree of acetylation in HPV16 early and late genes (Fig. 2A). We concluded that levels of histone H3 acetylation over the HPV16 genome, correlated with HPV16 gene expression levels.

Induction of histone H3 and H4 acetylation on the HPV16 genome correlates with activation of HPV16 gene expression in cervical cancer cells

To investigate if an increase in histone acetylation would enhance HPV16 late gene expression we screened a commercially available library of 21 HDAC inhibitors for induction of HPV16 late gene expression in the C33A2 reporter cell line. Three HDAC inhibitors named JNJ-26481585 (also known as quisinostat) (Qui) (Arts et al., 2009), panobinostat (Pano) (Atadja, 2009) and dual PI3K/HDAC inhibitor 1 (PI3KI) (Qian et al., 2012) induced HPV16 late gene expression which was monitored as elevated levels of sLuc activity in the cell culture medium of the C33A2 cells (Fig. 2B). The induced levels were higher than those induced by the positive control substance TPA (Fig. 2B) and the effect of the treatment peaked after 20 h of treatment (Fig. 2C). Combinations of the drugs revealed an additive effect on HPV16 late gene expression (Fig. 2D). All three substances caused a significant increase in acetylation of both histones H3 and H4 in the C33A2 cells (Fig. 2E). However, the dual HDAC- and PI3K-inhibitor PI3K/HDAC inhibitor I was less efficient than the others in inducing histone acetylation, in particular on histone H3 (Fig. 2E).

To investigate if the HDAC inhibitors affected acetylation of histones sitting on HPV16 DNA, C33A2 cells treated with either DMSO alone or DMSO with HDAC inhibitor quisinostat (Qui) were subjected to ChIP assays. The results revealed that the total levels of histone H3 and H4 associated with the HPV16 sequences were unaltered by the HDAC inhibitor as expected (Fig. 3A). The levels and distribution of the H3K9Ac histone mark were elevated in the early region of HPV16 as well as in the late region (Fig. 3A), and in particular over the E4 coding region (amplicon Enh#3) and in the beginning of L1 (amplicons SA5639 and L1) (Fig. 3A). In contrast, the levels and distribution of histone 4 acetylation, and the H4K8Ac and H4K16Ac marks specifically, were relatively

Fig. 2. (A) ChIP analyses on C33A2 cells using antibodies to proteins indicated in each histogram and qPCR of the indicated amplicons. Primers and antibodies are listed in Tables S1 and S2 respectively. Mean values with standard deviations of the amount of immunoprecipitated DNA compared to input DNA are displayed. For each antibody, the values for the CMVtata PCR is set to 1 to correct for differences between different ChIP extracts. White bars represent HPV16 early genes and gray bars represent late genes. *p*-Values were calculated for each ChIP result in relation to the CMVtata amplicon. *p*-Values less than 0.05 (*) or 0.01 (**) are indicated. All samples were analyzed in two independent ChIP assays and all qPCR reactions were performed in triplicates. (B) C33A2 cells were seeded in 96-well plates and incubated with the HDAC inhibitor library (Epigenetic Compound Library, L1900-01) (Selleckchem). Each inhibitor was tested in triplicates at a final concentration of 100 nM. Three inhibitors induced significant levels of sLuc from C33A2 cells: Inhibitor 1 (quisinostat/JNJ-26481585), inhibitor 3 (panobinostat) and inhibitor 19 (PI3K/HDAC inhibitor I/CUDC-907). All sLuc measurements were obtained from at least three independent cell treatments and were analyzed in triplicates. *p*-Values were calculated with sLuc results from each drug compared to sLuc results from C33A2 cells incubated with DMSO. *p*-Values less than 0.05 (*) or 0.01 (**) are indicated. (C) C33A2 cells were incubated with 100 nM of each HDAC inhibitor quisinostat (Qui), panobinostat (Pano) or PI3K/HDAC inhibitor I (PI3KI) and the sLuc activity was monitored in the cell culture medium at indicated time points after addition of drugs. Graph shows mean values and standard deviations of fold induction of sLuc activity of each drug compared to DMSO. All sLuc measurements were obtained from at least three independent cell treatments and were analyzed in triplicates. (D) C33A2 cells were incubated with 80 nM of each HDAC inhibitor quisinostat (Qui), panobinostat (Pano) or PI3K/HDAC inhibitor I (PI3KI), or combinations thereof, for 18 h. Graph shows mean values and standard deviations of fold induction of sLuc activity of each drug compared to DMSO. All sLuc measurements were obtained from at least three independent cell treatments and were analyzed in triplicates. *p*-Values were calculated with sLuc results from each drug compared to sLuc results from C33A2 cells incubated with DMSO. All *p*-values were less than 0.01(**), as indicated. (E) C33A2 cells were incubated with 80 nM of each HDAC inhibitor quisinostat (Qui), panobinostat (Pano) or PI3K/HDAC inhibitor I (PI3KI), or combinations thereof, for 18 h. Total protein extracts were analyzed by Western blotting with antibodies to the indicated proteins. The antibodies used are listed in Table S2.

unaffected by quisinostat (Qui) (Fig. 3A). We also investigated if the three HDAC inhibitors identified in the screen shown in Fig. 2B differed in their ability to induce acetylation of the HPV16 histones. While none of the inhibitors affected the overall levels or distribution of histones H3 or H4 over the HPV16 genome (Fig. 3B), panobinostat enhanced acetylation of H4K8 specifically

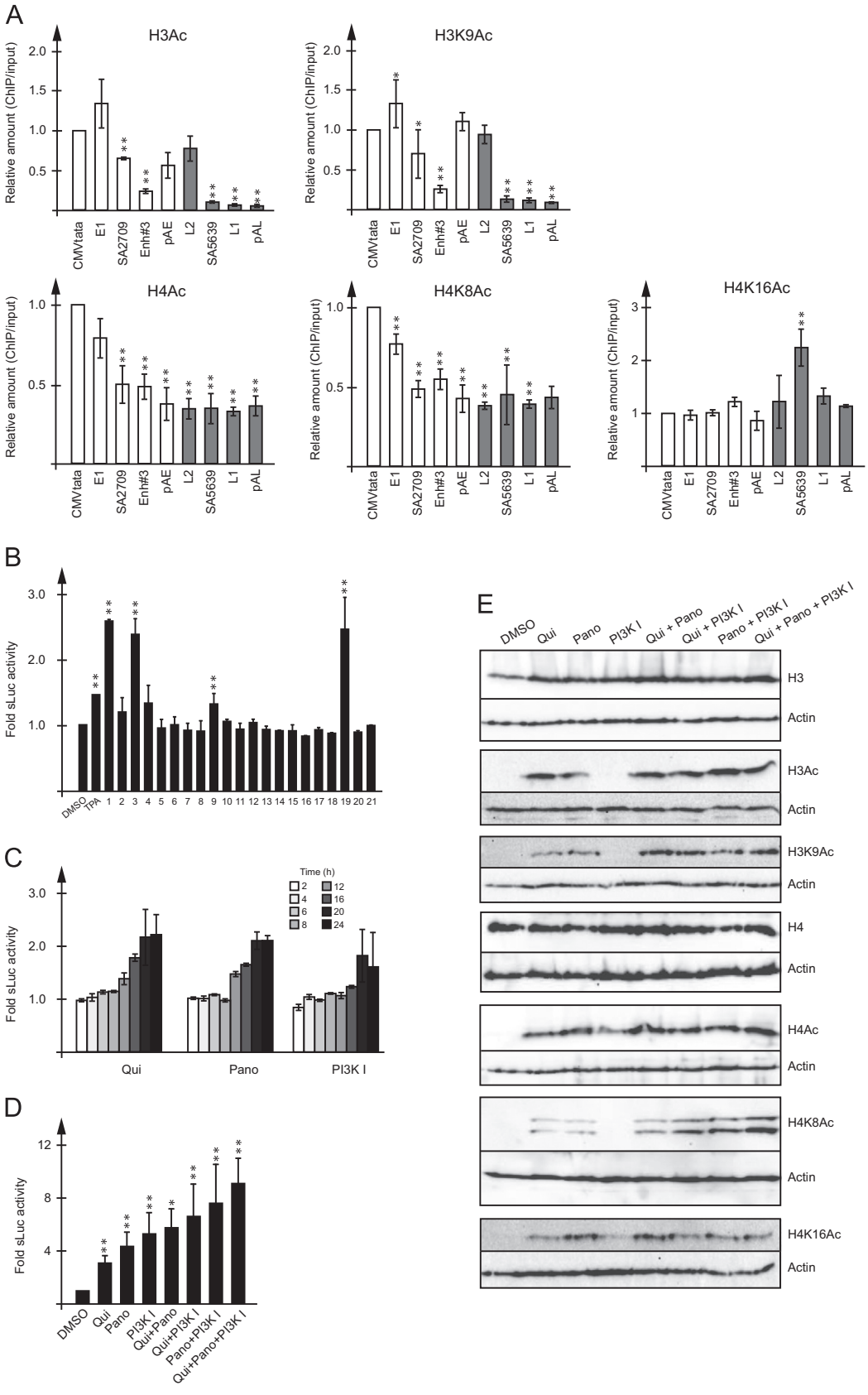

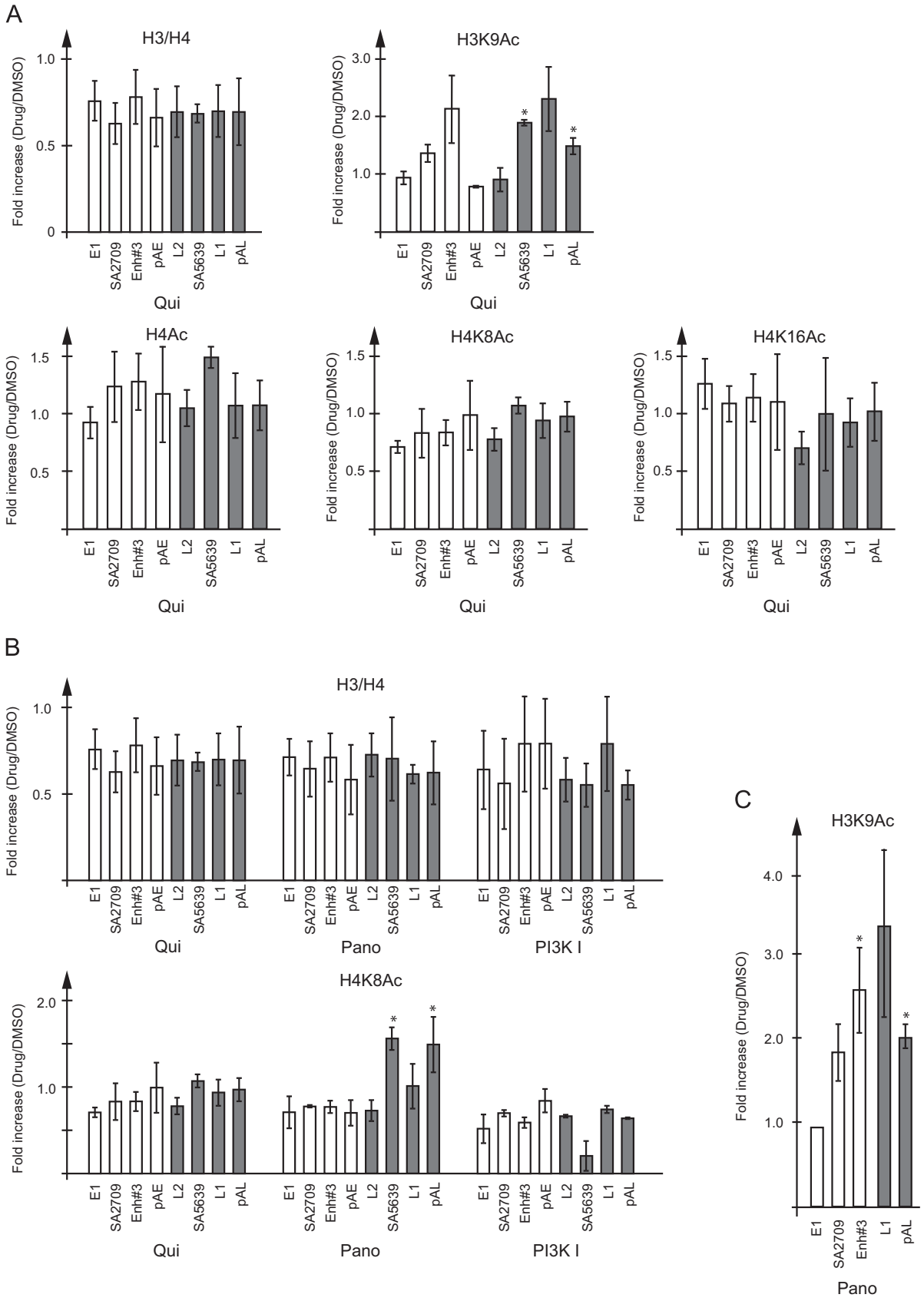

Fig. 3. (A–C) ChIP analyses on C33A2 cells treated with 80 nM of each HDAC inhibitor quisinostat (Qui), panobinostat (Pano) or PI3K/HDAC inhibitor I (PI3KI) using antibodies to proteins indicated in each histogram. qPCR of the indicated amplicons are displayed as fold over DMSO treated cells. *p*-Values were calculated for each ChIP result from cells treated with HDAC inhibitor in DMSO compared to cells treated with DMSO alone. *p*-Values less than 0.05 (*) or 0.01 (**) are indicated. Locations of amplicons in the HPV16 genome are shown in Fig. 1A and primers and antibodies are listed in Tables S1 and S2 respectively. Mean values with standard deviations are shown. All samples were analyzed in two independent ChIP assays and all qPCR reactions were performed in triplicates. White bars represent HPV16 early genes and gray bars represent late genes.

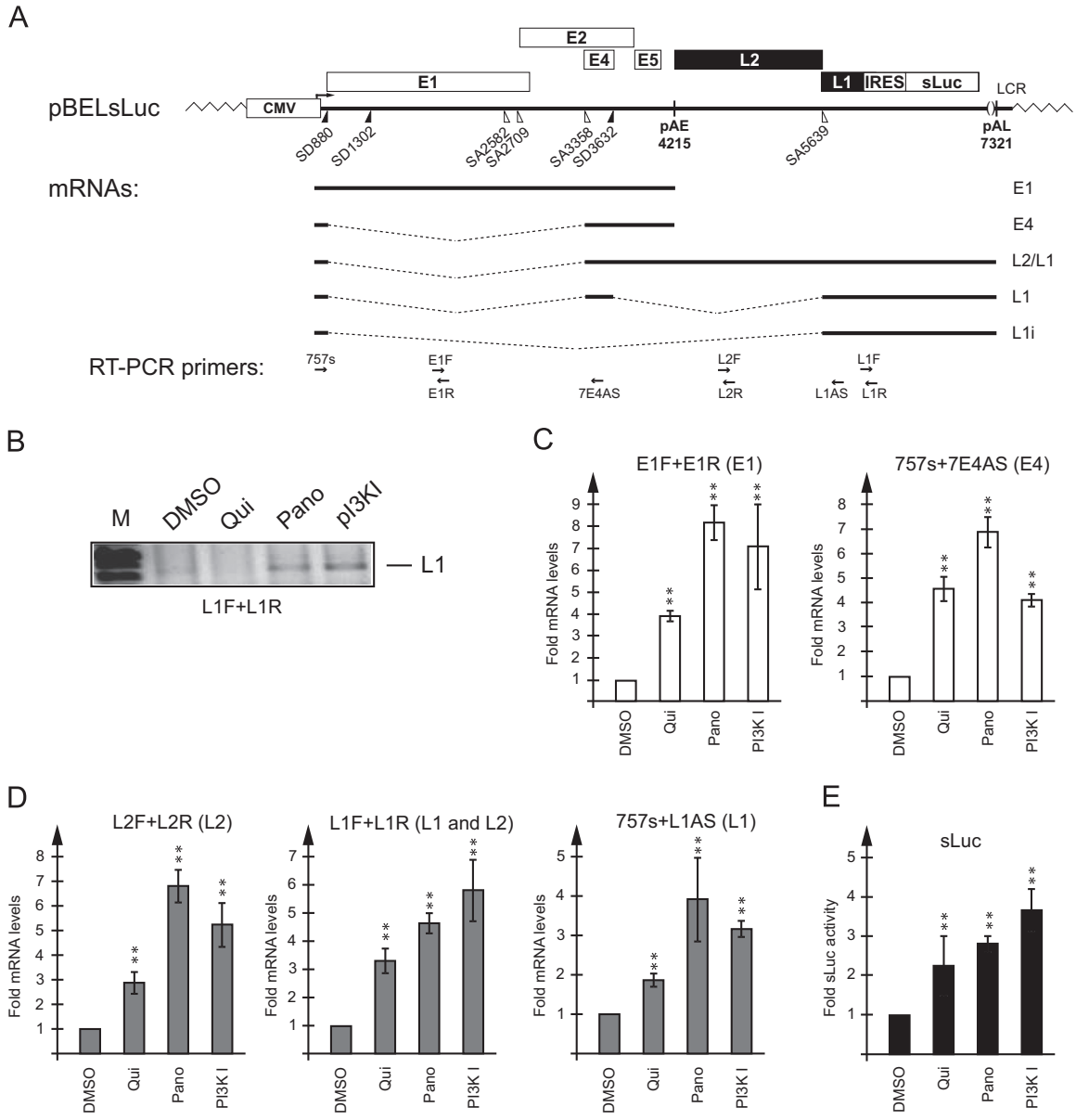

Fig. 4. (A) Schematic representation of the HPV16-derived pBELsLuc genomic construct (Li et al., 2013) stably integrated in the C33A2 reporter cells. A subset of the mRNAs produced by pBELsLuc is indicated and the primers used for RT-PCR are shown. (B) C33A2 cells were treated with 80 nM of quisinostat (Qui), panobinostat (Pano) or PI3K inhibitor I (PI3K) DMSO as a control. Total RNA was extracted after 20 h of incubation and was subjected to RT-PCR with the indicated L1F and L1R primers. RT-PCR primers are listed in Table S3. (C) RT-qPCR on cDNA of HPV16 early mRNAs and (D) late mRNAs with the indicated primer pairs. Graphs show fold mRNA induction for each HDAC inhibitor compared to DMSO from a total of three different experiments. HPV16 mRNA levels were normalized to GAPDH mRNA levels. All RNA analyses were performed on at least three independent RNA preparations with RT-qPCR performed in triplicate reactions. *p*-Values were calculated with RT-qPCR results on RNA from cells treated with each drug compared to RT-qPCR results from C33A2 cells incubated with DMSO. All *p*-values were below 0.01 (**) as indicated. (E) sLuc activity in the cell culture medium at the time of RNA harvest. Graph shows mean values and standard deviations of fold sLuc activity induced by each inhibitor compared to DMSO from five independent experiments. *p*-Values were calculated with sLuc results from each drug compared to sLuc results from C33A2 cells incubated with DMSO. All *p*-values were below 0.01 (**) as indicated.

in the late region of HPV16 (Fig. 3B). Furthermore, abundance of H3K9Ac on HPV16 early and late genes increased with both Qui (Fig. 3A) and Pano (Fig. 3C). We concluded that treatment of C33A2 cells with HDAC inhibitors could increase acetylation of H3 and H4 histones in early and late regions of the HPV16 genome. This increase in histone acetylation on the HPV16 genome was accompanied by an increase in HPV16 early and/or late gene expression.

Next we measured the effect of the HDAC inhibitors on the various alternatively spliced HPV16 mRNAs produced in the C33A2 reporter cell line (Fig. 4A). Since sluc levels were induced by the HDAC inhibitors, we first monitored levels of L1 mRNAs by standard, end-point RT-PCR (Fig. 4B). While L1 mRNA levels induced by Pano and PI3KI were readily detected, detection of L1 mRNA levels induced by quisinostat (Qui) required 2–4 more PCR cycles (Fig. 4B). To assess HPV16 mRNA production more reliably after incubation with HDAC inhibitors, HPV16 early mRNAs (E1 and E4) and late mRNAs (L2 and L1 or, L2 and L1 combined) were monitored by RT-qPCR (Fig. 4C). The RT-qPCR assay was performed on RNA extracted from C33A2 cells incubated in the absence (DMSO-treated) or presence of either of the three inhibitors quisinostat (Qui), panobinostat (pano) or PI3K/HDAC inhibitor 1 (PI3KI). The results revealed that the HDAC inhibitors enhanced expression of HPV16 early and late mRNAs. The increase in the HPV16 early E1 and E4 mRNAs was roughly four- to eight-fold (Fig. 4C), while the increase in the late L2 or L1 mRNAs combined was approximately three- to seven-fold (Fig. 4D). The induction of

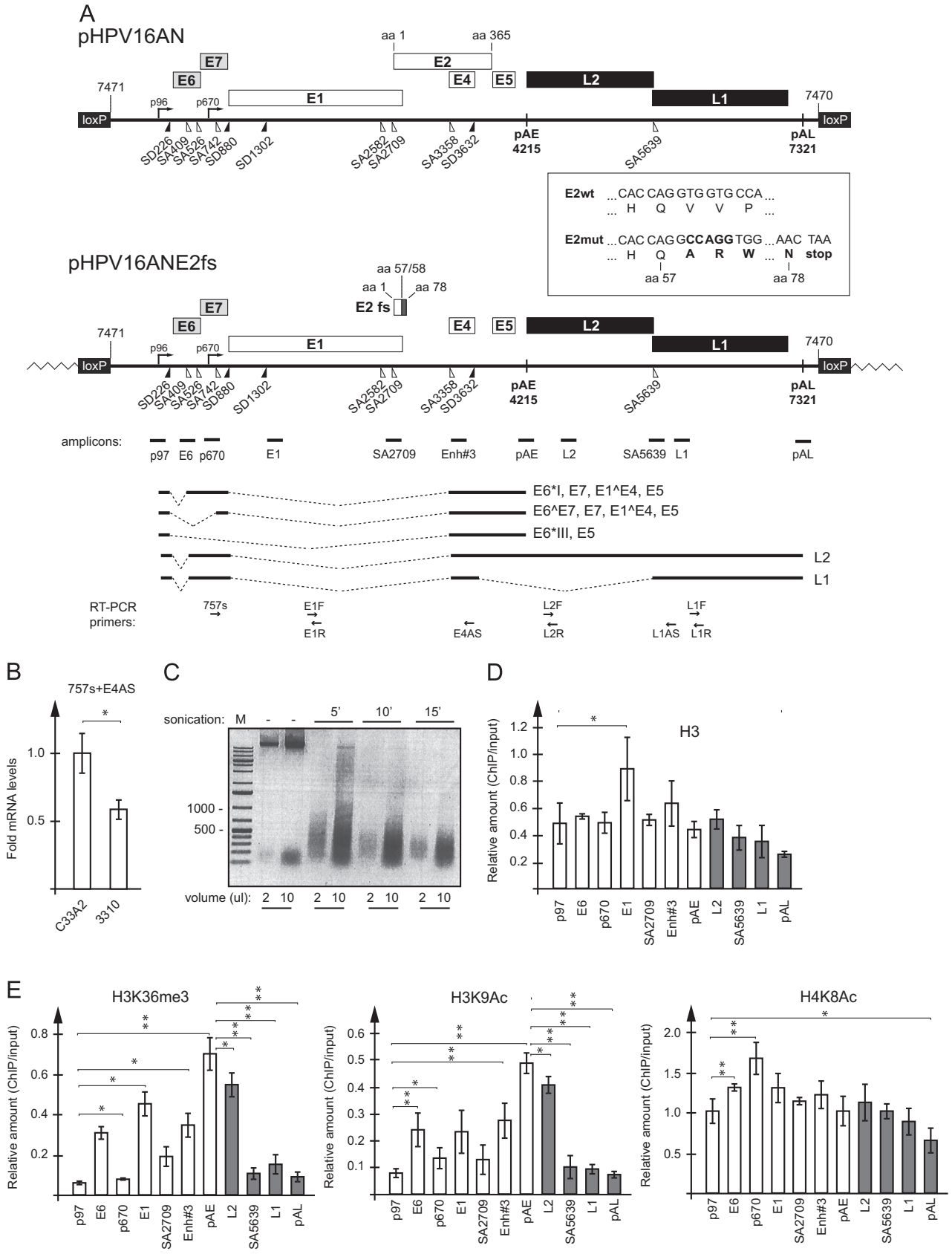

spliced HPV16 L1 mRNAs was slightly lower and was in the range of two- to four-fold (Fig. 4D), suggesting that the HDAC inhibitors affected read-through at pAE rather than L1 mRNA splicing. The HDAC inhibitors induced sLuc production in the same cells, as expected (Fig. 4E). We concluded that the HDAC inhibitors increased histone acetylation on both HPV16 early and late genes and that this induction correlated with activation of both HPV16 early and late gene expression.

Low levels of H3K36me3 and H3K9Ac in the late region of HPV16 in HPV16-immortalized cells

Since the experiments above were all performed in cervical cancer cells, we wished to study cells representing earlier stages of the HPV16 infection. We therefore transfected human primary keratinocytes with a plasmid encoding the full HPV16 genome (pHPV16AN (Fig. 5A)) to obtain immortalized cell lines. Unfortunately, all cells transfected with HPV16 genomic plasmids encoding the HPV16 wild type E2 gene integrated into the chromosomes of the keratinocytes, in or near the HPV16 E2 gene. Thus, these cells could not be used to study the effect of HDAC inhibitors on HPV16 early and late gene expression. We therefore transfected the primary keratinocytes with an HPV16 E2-negative mutant of HPV16 (pHPV16ANE2fs) in which a frame shift mutation was introduced at amino acid position 58 in E2 (Fig. 5A). This mutation did not affect any other HPV16 gene. A cell clone named 3310 in which pHPV16ANE2fs was integrated in the TOPO vector part of the plasmid and not in E2 was selected (data not shown). The integrated HPV16 genome in cell clone 3310 could be transcribed in its entirety and the epigenetic properties of both HPV16 early and late gene expression could be investigated. However, any role of HPV16 E2 in then epigenetic regulation of HPV16 gene expression would be missed. Cell clone 3310 produced similar levels of HPV16 early mRNAs spliced between SD880 and SA3358 as the C33A2 reporter cell line (Fig. 5B), whereas late mRNA levels were low.

We performed a ChIP analysis on chromatin preparations from the 3310 cells that contained primarily monosomes (Fig. 5C). As expected, histone H3 showed a relatively even distribution over HPV16 early and late genes, although a peak of H3 histones was observed in the E1 region (Fig. 5D). Interestingly, both H3K36me3 and H3K9Ac marks were rare in the late region of the HPV16 genome in the HPV16 immortalized 3310 cells (Fig. 5E), which is in agreement with the results obtained with cervical cancer derived C33A2 reporter cell line (Figs. 1E and 2A). These marks were higher in the early and middle regions of the HPV16 genome, with the exception of the p97 and p670 promoter regions (Fig. 5E). In contrast, H4K8Ac was more evenly distributed over the entire HPV16 genome in the 3310 cells (Fig. 5E), which is also in agreement with results obtained in the C33A2 cells (Fig. 2A). We concluded that the pattern of histone marks on HPV16 was similar in cervical cancer cells and in HPV16 immortalized human keratinocytes.

Increased acetylation of histones on the HPV16 genome induces HPV16 early and late gene expression in HPV16 immortalized cells

Since the H3K9Ac was low in the HPV16 late region compared to the early region, we speculated that addition of HDAC inhibitors may affect histone acetylation in the HPV16 genome, thereby inducing HPV16 late gene expression. Addition of the same three HDAC inhibitors that induced HPV16 late gene expression in the C33A2 cells: JNJ-26481585/quisinostat (Qui), panobinostat (Pano) and PI3K/HDAC inhibitor I (PI3KI) caused an increase in global cellular histone acetylation in the 3310 cells (Fig. 6A). The results were similar to those obtained with the C33A2 cells, i.e. Qui and Pano efficiently induced histone acetylation whereas PI3KI did so to a lesser extent (Fig. 6A). Total histone H3, H4 or actin levels were unaltered by the HDAC inhibitors (Fig. 6A). Furthermore, none of the methylation inhibitors had any detectable effect on HPV16 gene expression in the 3310 cells.

Next we investigated if the HDAC inhibitors affected acetylation of histones on the HPV16 genome. These experiments were performed with HDAC inhibitor JNJ-26481585/quisinostat (Qui). As expected, the levels of histone H4 over the HPV16 genome were relatively unaffected by HDAC inhibitor Qui (Fig. 6B), while the total levels of acetylated H4 (H4Ac) increased dramatically (up to 45-fold) (Fig. 6C). This increase was particularly apparent in the HPV16 promoter region and over the HPV16 late genes (Fig. 6C). Part of the increase in acetylated H4 was attributed to increased acetylation of H4K8 as H4K8Ac increased around 10-fold over the entire HPV16 genome (Fig. 6C), while the levels of H4K16Ac were relatively unaltered (around 1.5-fold increase) (Fig. 6C). Acetylation of H3K9 over the HPV16 genome also increased dramatically by HDAC inhibitor treatment and resulted in an up to 17-fold increase of H3K9Ac in the late region of the HPV16 genome (Fig. 6C). Similarly to H4Ac, the increase in H3K9Ac was highest at the HPV16 promoter region and in the late region of the HPV16 genome, while histone acetylation in the E1 region was unaffected (Fig. 6C). These results suggested that histone acetylation could potentially affect HPV16 gene expression in the HPV16 immortalized 3310 cells.

To investigate if the HDAC inhibitors also affected HPV16 gene expression in the HPV16 immortalized 3310 cells, they were treated with the three HDAC inhibitors JNJ-26481585 Quisinostat/Qui, Panobinostat (Pano) and PI3K/HDAC inhibitor 1 (PI3K1). The results revealed that the HDAC inhibitors Qui and Pano caused a two-to-three-fold induction of HPV16 early E1 and E4 mRNAs, whereas HDAC inhibitor PI3KI caused a six-fold induction of both E1 and E4 mRNAs (Fig. 6D). However, HPV16 late gene expression was only induced to a minor extent (less than two-fold) (Fig. 6D). This effect was only seen with primers in the L2 coding region and not with primers detecting spliced L1 mRNAs (Fig. 6D), suggesting that the HDAC inhibitors caused a read-through at the HPV16 pAE rather than an increase in HPV16 late mRNA splicing. We concluded that increased histone acetylation over the HPV16 genome correlated with an increase in HPV16 early and late gene expression.

Discussion

A number of histone marks have been shown previously to be enriched over cellular DNA sequences coding for exons in cellular genes including H3K36me3, H3K27me1, H3K27me2, H3K27me3, H3K79me1, H4K20me1 and H2BK5me1 (Barski et al., 2007; Wagner and Carpenter, 2012; Spies et al., 2009; Andersson et al.,

Fig. 5. (A) Schematic representation of the HPV16 genome in wild type HPV16 plasmid pHPV16AN (Li et al., 2013) and E2-negative mutant pHPV16ANE2fs. The frame-shift mutation in E2 is indicated. Open reading frames are depicted as rectangles. Early and late promoters p97 and p670, respectively, are indicated as arrows and splice sites as triangles. The long control region (LCR) and the early and late polyA signals pAE and pAL are indicated. The pHPV16ANE2fs plasmid is integrated in the genome of the HPV16-immortalized 3310 cells in such a way that the entire HPV16 genome could potentially be transcribed from the HPV16 p97 promoter. The location of each amplicon used for ChIP analyses is shown. A subset of the HPV16 early mRNAs produced from pHPV16ANE2fs in the 3310 cells is indicated, as well as RT-PCR primers. ChIP primers and RT-PCR primers are listed in Tables S1 and S3, respectively. (B) The levels of early mRNA spliced from SD880 to SA3358 in the 3310 cells were monitored by RT-qPCR with primers 757s and E4AS and compared to the levels of the same amplification production from the C33A2 reporter cell line. Fold difference is shown and (*) indicates a *p*-value of less than 0.05. (C) Optimization of sonication conditions to obtain primarily mononucleosomes from the chromatin preparations from 3310 cells. (D, E) ChIP analyses on 3310 cells using antibodies to histone marks indicated in each histogram. Mean values with standard deviations of the amount of immunoprecipitated DNA compared to input DNA are displayed. qPCR of the indicated amplicons are displayed. Primers and antibodies are listed in Tables S1 and S2 respectively. Mean values with standard deviations are shown. qPCR of the indicated amplicons are displayed as fold over DMSO treated cells. All samples were analyzed in two independent ChIP assays and all qPCR reactions were performed in triplicates. *p*-Values were calculated for each ChIP result in relation to either the p97 amplicon or the pAE amplicon as indicated in the figure. *p*-Values less than 0.05 (*) or 0.01 (**) are indicated. White bars represent HPV16 early genes and gray bars represent late genes.

2009). One could therefore speculate that these histone marks might accumulate in the early region of HPV16, perhaps in particular downstream of the efficiently used HPV16 3′-splice site SA3358. Of these histone marks, we found that H2BK5me1 was enriched in the late region of HPV16 and as such displayed an inverse correlation with HPV16 gene expression levels. H3K27me3 and H4K20me1 on the other hand were evenly distributed over HPV16 early and late genes. We concluded that none of the histone marks monitored here were enriched over efficiently used exons on HPV16. Other histone marks have been shown to be enriched over exons and to recruit splicing factors and/or RNA binding proteins, presumably to enhance chances of splicing silencer or splicing enhancer recognition by splicing regulatory proteins. For example, H3K36me3 binds the Psip1/Ledgf p52 protein that recruits the splicing stimulatory proteins ASF/SF2 (SRSF1) and SRp20 (SRSF3) (Pradeepa et al., 2012), while under other circumstances H3K36me3 interacts with MRG15 that recruits the splicing inhibitory factor polypyrimidine tract binding protein (PTB) (Luco et al., 2010). The presence or absence of H3K36me3 may therefore either promote or inhibit splicing depending on whether SR proteins or PTB is recruited. In the experiments reported here, we found that H3K36me3 was rare in the late region compared to the early region perhaps contributing to inefficient splicing to SA5639 by lack of recruitment of SR proteins to the HPV16 late region. However, we were unable to provide support for the idea that low levels of H3K36me3 in the HPV16 late region prevents HPV16 late gene expression as all histone de-methylase inhibitors used here failed to affect HPV16 gene expression. H3K9me3 on the other hand was more common over the HPV16 late region than over the HPV16 early genes. This is in contrast to other reports suggesting that H3K9me3 is enriched on alternatively spliced exons under conditions that lead to their inclusion in mRNA (Saint-Andre et al., 2011). Since inhibitory RNA elements in the HPV16 late region interact with hnRNP proteins hnRNPA1, hnRNPA2/B1, hnRNPAB, hnRNPD, hnRNPDL, hnRNPE, hnRNPH and hnRNPK (Zhao et al., 2004; Li et al., 2013; Oberg et al., 2005; Collier et al., 1998), and it has been shown that H3K9me3 interacts with hnRNPA1, hnRNPA2/B1, hnRNPAB, hnRNPK and hnRNPL (Vermeulen et al., 2010), one may speculate that H3K9me3 recruits hnRNPs to the late mRNAs thereby contributing to suppression of HPV16 late gene expression. This is not without precedence since both H3K36me3 and H2A.Bbd interact directly or indirectly with a number of hnRNPs (Pradeepa et al., 2012; Tolstorukov et al., 2012). Similarly to H3K9me3, both H2BK5me1 and H4K20me3 were enriched over the HPV16 late region demonstrating an inverse correlation with HPV16 gene expression. It remains to be determined if the HDAC inhibitors act on HPV16 transcription or RNA processing or both to induce HPV16 gene expression.

In neuronal cells, hyperacetylation of H3K9 (H3K9Ac) over exon 18 in the neural cell adhesion molecule (NCAM) gene, and histone H3 and H4 hyperacetylation of exon 23a in the neurofibromatosis-1 gene and exon 6 of the Fas gene correlates with exon skipping (Zhou et al., 2011; Schor et al., 2009). Enhanced transcription, recruitment of splicing inhibitory factors, and lack of recruitment of splicing stimulatory factors have been suggested to explain the results. In our experiments, a low concentration of acetylated H3K9 is observed in the late region of the HPV16 genome and invariably correlates with low HPV16 gene expression in both cervical cancer cells and in immortalized human keratinocytes. In contrast, acetylation of histone H4 is more evenly distributed over the HPV16 genome, with the exception of H4K16Ac that is more abundant at HPV16 late L1 splice site SA5639. Treatment of C33A2 cervical cancer cells or HPV16-immortalized 3310 cells with HDAC inhibitors caused an increase in H4Ac, H4K8Ac, and H3K9Ac over the entire HPV16 genome in the 3310 cells, or in the late region specifically in the C33A2 cells. This increase correlated with an increase in HPV16 early and late mRNA levels, but did not alter alternative splicing of HPV16 mRNAs. However, induction of HPV16 late gene expression was more efficient in the C33A2 cells than in the 3310 cells, despite a much more pronounced effect on histone acetylation over the HPV16 genome in 3310 cells than in C33A2 cells. In contrast, levels of H4K16Ac on the HPV16 genome were unaffected by the HDAC inhibitors used here, despite a global increase in H4K16Ac by the HDAC inhibitors. We concluded that an increase in H3K9Ac and H4K8Ac on the HPV16 genome correlated with an increase in HPV16 gene expression. Although the increase in histone acetylation on the HPV16 genome did not specifically alter HPV16 mRNA splicing, it did allow increased HPV16 late gene expression, including production of HPV16 L2 mRNAs and spliced L1 mRNAs, strongly suggesting that HPV16 splicing and/or polyadenylation were affected by epigenetic changes on the HPV16 genome.

A peak in histone H3 acetylation over the HPV16 early polyA signal pAE was apparent, in particular for H3K9Ac, whereas acetylation of histone H4 appeared to be indifferent to the presence of the polyA signal. It has been shown that the HuR protein can bind HDACs and inhibit their enzymatic activities, thereby functioning as a local HDAC inhibitor (Zhou et al., 2011). We have previously shown that overexpression of HuR can induce HPV16 late gene expression (Johansson et al., 2012). It is not unreasonable that HuR binds to the U-rich region in the HPV16 early UTR and acts by preventing HDACs from de-acetylating histone H3 at pAE. Polyadenylation may also be controlled by histone modifications (Spies et al., 2009). High levels of HuR would produce an acetylated zone at pAE, which presumably would have an impact on the polyadenylation efficiency at pAE, and thereby contributing to the regulation of the switch from HPV16 early to late gene expression.

HDACs were originally shown to control transcription and high levels of acetylated histones are common at active promoters as they open up the chromatin and allow access to transcription factors that control transcription initiation. It is therefore conceivable that HDAC inhibitors used here affected the promoters of the reporter construct and/or the HPV16 genomes. However, induction of HPV16 early and late gene expression in the reporter cell line C33A2 is not controlled solely at the level of transcription since replacing the viral late promoter p670 that is silent in mitotic cells, with the highly active CMV promoter does not cause induction of HPV16 late gene expression (Zhao et al., 2004). However, treatment of the C33A2 cells with HDAC inhibi-

Fig. 6. (A) C33A2 and 3310 cells were treated with 80 nM of Quisinostat (Qui), Panobinostat (Pano) and a PI3K inhibitor (PI3K) (alone or in combinations, as indicated) for 18 h. DMSO was used as control. Total protein extracts were analyzed by Western blotting with antibodies to the indicated proteins. Antibodies are listed in Table S2. (B, C) ChIP analyses on 3310 cells treated with 80 nM of each HDAC inhibitor quisinostat (Qui), panobinostat (Pano) or PI3K/HDAC inhibitor I (PI3KI) using antibodies to proteins indicated in each histogram. qPCR of the indicated amplicons are displayed as fold over DMSO treated cells. Locations of amplicons in the HPV16 genome are shown in Fig. 5A and primers and antibodies are listed in Tables S1 and S2 respectively. Mean values with standard deviations are shown. All samples were analyzed in two independent ChIP assays and all qPCR reactions were performed in triplicates. White bars represent HPV16 early genes and gray bars represent late genes. *p*-Values were calculated for each ChIP result from cells treated with HDAC inhibitor in DMSO compared to cells treated with DMSO alone. *p*-Values less than 0.05 (*) or 0.01 (**) are indicated. (D) The HPV16 immortalized 3310 cells were treated with 80 nM of quisinostat (Qui), panobinostat (Pano) or PI3K/HDAC inhibitor I (PI3KI) for 18 h followed by total RNA extraction. DMSO was used as control. RT-qPCR on cDNA of HPV16 early mRNAs (white bars) and late mRNAs (gray bars) was performed with the indicated primer pairs. Graphs show fold mRNA induction for each inhibitor compared to DMSO from a total of three different experiments. HPV16 mRNA levels are normalized to GAPDH mRNA levels. RT-qPCR primers are listed in Table S3. Mean values with standard deviations are shown. All RNA analyses were performed on at least three independent RNA preparations with RT-qPCR performed in triplicate reactions. *p*-Values were calculated for each RT-qPCR result obtained in the presence of drug compared to DMSO treatment cells. *p*-Values less than 0.05 (*) or 0.01 (**) are indicated.

tors does. This correlates with an increase in histone acetylation in both HPV16 early and late genes, suggesting that an overall increase in histone acetylation is required for induction of HPV16 late gene expression. Our results therefore suggest that acetylation of intragenic histones contribute to the control of HPV16 gene expression.

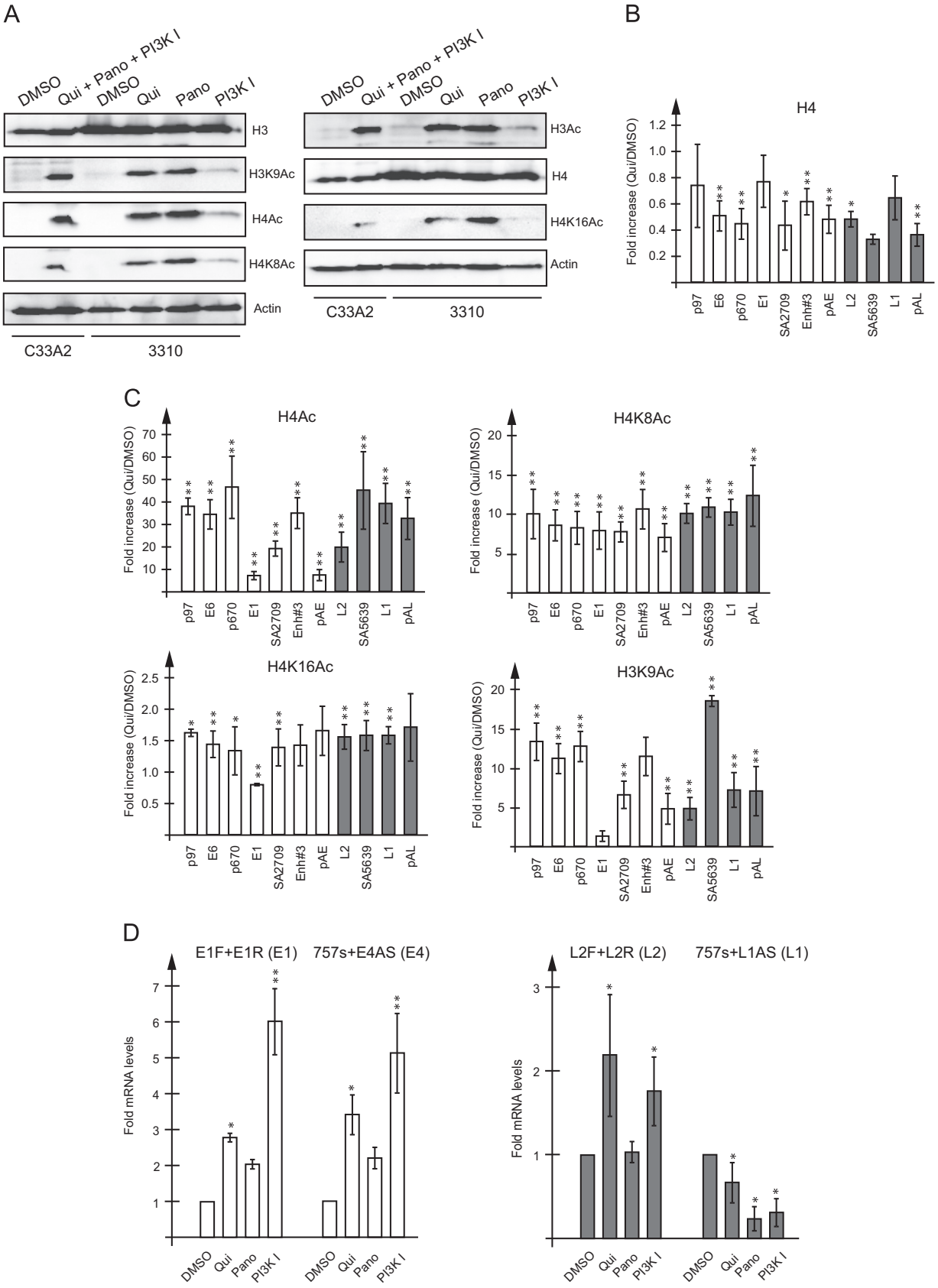

HPV31 E7 has been shown to bind to HDACs and inhibit their function (Longworth and Laimins, 2004). However, E7 is not expressed in the C33A2 reporter cell line and is therefore not interfering with gene expression results or acetylation of internal histones in the HPV16 genome. However, the 3310 cells were immortalized by HPV16 and therefore have been selected for HPV16 E6 and E7 expression. Interestingly, the pattern of histone acetylation over the HPV16 genome in the cervical cancer cell line C33A2 and the immortalized keratinocyte cell line 3310, is very similar, including relatively low histone acetylation in HPV16 early and late genes and a high peak in histone acetylation at and around the HPV16 early polyA signal pAE. Therefore, interactions of E7 with HDACs do not seem to interfere with histone acetylation of HPV16 induced by the small molecule HDAC inhibitors used here. However, since HDACs acetylate a variety of cellular proteins, not just histones (Martinez-Redondo and Vaquero, 2013), we cannot exclude that the induction of HPV16 gene expression is the effect of acetylation of cellular protein(s) that are more directly involved in gene regulation than histones.

Certain histone marks are associated with cancer and loss of H4K16Ac and H4K20me3 appears to be a hallmark of cancer (Fraga et al., 2005). H4K16Ac and H4K20me3 were found in normal keratinocytes, but were lost in benign papillomas, suggesting that the loss of these two marks may occur early in the carcinogenic process (Fraga et al., 2005). We did not detect differences in levels of H4K16Ac between C33A2 cervical cancer cells and the HPV16-immortalized 3310 cells, neither was H4K16Ac affected by the HDAC inhibitors used here. However, both H4K16Ac and H4K20me3 were more prevalent in the HPV16 late region than in the early region in the cervical cancer cell line C33A2, whereas H4K16Ac was evenly distributed over the HPV16 genome in the immortalized 3310 cells. Progression of HPV16 infection to cervical cancer could potentially be associated with changes of H4K16Ac and H4K20me3 over the HPV16 genome, in particular in the late region. It would be of interest to investigate if the histone marks that correlate with HPV16 gene expression levels such as H3K9me3, H3K36me3, H2BK5me1 and H3K9Ac show a similar pattern over HPV16 in HPV16 infected individuals. In particular, one may investigate if the HPV16 landscape of histone marks changes in response to disease progression and if it correlates with severity of the premalignant cervical lesions.

While quisinostat and panobinostat are HDAC-specific inhibitors (Arts et al., 2009; Atadja, 2009), PI3K/HDAC inhibitor I is a dual inhibitor that inhibits both HDACs and the PI3K-kinase in the PI3K/AKT pathway (Qian et al., 2012). Since the dual inhibitor PI3K/HDAC inhibitor I was less efficient than quisinostat and panobinostat in inducing histone acetylation in the C33A2 cells and in the 3310 cells, but induced HPV16 late gene expression to a similar extent as quisinostat and panobinostat, one may speculate that other effects on the cells of PI3K/HDAC inhibitor I contributed to the efficient induction of HPV16 late gene expression. It will therefore be of interest to investigate if the PI3K/AKT pathway controls HPV16 gene expression. The apparently lower effect of the PI3KI inhibitor on histone acetylation observed here may also be explained by a previously described time-dependent effect of the PI3KI substance on histone acetylation (Qian et al., 2012). Furthermore, it has been reported that selective induction of apoptosis by panobinostat in cancer cells, and not in normal cells, correlated with increased acetylation of histones (Atadja, 2009). However, an increase in histone acetylation also occurred in the normal cells, suggesting that panobinostat may act on other cellular proteins as well (Atadja, 2009). Panobinostat also induces acetylation of hsp90 and as a consequence, causes a decrease in the levels of phosphorylated AKT (Atadja, 2009). Taken together, one may speculate that the PI3K/AKT pathway controls HPV16 gene expression.

It has been suggested that HDACs promote viral latency, for example by de-acetylating and silencing the human immunodeficiency virus type 1 (HIV-1) long terminal repeat (LTR) promoter (Matalon et al., 2011). HDAC inhibitors may therefore be used to chase latent viruses such as HIV-1 and 2, Epstein Barr virus (EBV) and herpes simplex types 1 and 2 out of the latency state to sensitize these infections to antiviral therapy (Ghosh et al., 2012). It has previously been shown that HDAC inhibitors sodium butyrate and trichostatin A arrested HeLa cells as well as HPV16 E6/E7 immortalized keratinocytes in G1 to S-transition (Finzer et al., 2001), and recently HDAC inhibitor vorinostat was reported to inhibit growth of an HPV11-positive pulmonary tumor in vivo in one patient (Yuan et al., 2012). One may speculate that HDAC inhibitors could be used to induce premature late gene expression in HPV infected cells or in high grade lesions at risk of progressing to cancer, thereby uncovering the infected cells for the immune system of the host that could potentially clear the HPV infection. However, as HDAC inhibitors also induce expression of the early genes encoding the E6 and E7 oncogenes, treatment of cervical cancer with or high-grade lesions with HDAC inhibitors could potentially be contra productive.

Materials and methods

Cell culture

The C33A2 reporter cell line will be described elsewhere. Briefly, it is derived from the HPV-negative, human cervical carcinoma cell line C33A, which was stably transfected with the subgenomic reporter plasmid pBELsluc. C33A2 cells are maintained in Dulbecco's modified Eagle medium containing 10% bovine calf serum and penicillin-streptomycin.

The 3310 cell line will be described elsewhere. Briefly, it is derived from neonatal human epidermal keratinocytes (HEKn) purchased from Gibco Invitrogen Cell Culture stably transfected with plasmid pHPV16ANE2fs encoding an E2-negative, HPV16 full-length genome. Briefly, immortalized, G418-resistent colonies were selected and characterized to obtain a cell clone that contains the entire HPV16 genome integrated in such a way that the HPV16 genome is uninterrupted. This resulted in the 3310 cell line. The 3310 cell line is propagated in EpiLife Medium supplemented with Human keratinocyte Growth Supplement (Gibco Invitrogen Cell Culture) as recommended by the manufacturer. The primary keratinocytes are grown in monolayer cultures and expanded under growth conditions that maintain poorly differentiated cells with properties similar to the cells in the basal layers of the epithelium.

Inhibitors

The HDAC inhibitor library (Epigenetic Compound Library, L1900-01) was purchased from Selleckchem. Cell culture medium was replaced with medium containing indicated concentrations of inhibitor or with 80 nM each of the three different HDAC inhibitors quisinostat (JNJ-26481585) (Arts et al., 2009), panobinostat (Atadja, 2009) and PI3K/HDAC inhibitor I (CUDC-907) (Qian et al., 2012) for indicated time periods. DMSO was used as a control. The following histone de-methylase inhibitors were used at 50 μM as indicated in each figure legend: JMJD3 and UTX inhibitor GSKJ4-HCl (S7070 Selleckchem), LSD1 inhibitor OGL-002 (S7237 Selleckchem), tranylcypromine (2-PCPA) (S4246 Selleckchem), JMJD2 inhibitors N-Oxalylglycine (NOG) (O9390 Sigma), 5-Carboxy-8-hydroxyquinoline (CHQ) (SML0067 Sigma) and ML324 (Axon 2081 Axon Medchem). The following DNA methyltransferase inhibitors were used at concentrations indicated in each figure legend: azacytidine (A2385

Sigma), RG108 (R8279 Sigma). All inhibitors were dissolved in DMSO, and DMSO in the absence of inhibitor was used as a control in all experiments.

Secreted Luciferase assay

The secreted Luciferase activity in the medium of the cells was measured with the Ready To Glow Secreted Luciferase Reporter assay (Clontech). The collected media was centrifuged at 14,000*g* for 5 min, 50 µl of cell culture media was mixed with 50 µl PBS and 5 µl 0.5 × Luciferase substrate in Reaction buffer. The luminescence was measured in a Tristar Luminometer (Berthold Technologies).

Western blotting

C33A2 and 3310 cells were lysed using RIPA-buffer (50 mM Tris pH 7.8, 300 mM NaCl, 1% Na-deoxycholate, 0.1% SDS, 1% Triton X-100 and protease inhibitors). The 3310 cells were also subjected to sonication. The protein concentration of each cell extract was determined and equal amounts of proteins were separated on SDS-PAGE gels and transferred to nitrocellulose membranes. Membranes were incubated with primary antibodies to various histones or actin (Table S2) and Horseradish peroxidase-conjugated secondary antibody (Sigma). The bands were visualized using The SuperSignal West Pico and Femto Chemiluminescent Substrates and images captured with the ChemiDoc MP System (BioRad).

RNA extraction and reverse transcription

Total RNA was extracted by Tri reagent (Sigma) according to manufacturers protocol. The RNA was DNase-treated and reprecipitated. Two to five hundred nanograms of total RNA was reverse transcribed to cDNA in a 25 µl reaction at 42 °C by using random hexamers and MLV Reverse Transcriptase (Invitrogen) according to the manufacturer's instructions. RT-PCR primers are listed in Table S3.

Quantitative PCR

Quantitative PCR was performed on cDNA or purified ChIP DNA using the SsoAdvanced SYBR Green Supermix (BioRad) according to the manufacturer's instructions. Primer sequences are shown in Tables S1 and S3. Cycling was performed in the MiniOpticon System (BioRad). Obtained Ct values were used to calculate the amount of each immunoprecipitation relative to the input according to: Relative amount $=2^{-Ct(IP)}/2^{-Ct(input)}$, for each PCR amplicon. For drug treatments, the fold change compared to DMSO-treated samples was calculated according to Fold change $=(2^{-Ct(IP)}/2^{-Ct(input)})_{drug}/(2^{-Ct(IP)}/2^{-Ct(input)})_{DMSO}$.

Me-DNA immunoprecipitation

C33A2 cells were lysed in 10 mM Tris pH 8.0, 100 mM NaCl, 25 mM EDTA, 0.5% SDS and 250 µg/ml proteinase K by overnight incubation at 50 °C. Purified DNA was RNase-treated, ethanol-reprecipitated and dissolved in TE buffer. The DNA was sonicated 10–15 × 30 s in a Diagenode Bioruptor with high setting to achieve DNA shearing to approximately 500–1500 bp fragments. Four micrograms of sonicated DNA diluted to 450 µl in TE buffer was used for each immunoprecipitation. The DNA was denatured at 95 °C for 10 min after which 50 µl 10 × IP buffer (100 mM Na-phosphate, pH 7.0, 1.4 M NaCl, 0.5% Triton X-100) was added. Me-C or control IgG antibodies were added and incubated for 2–4 h at 4 °C. Immune complexes were precipitated by a 2 h end-over-end incubation at 4 °C with Protein G Magnetic Beads. Beads were washed three times with 1 × IP buffer. Samples were eluted from the beads with elution buffer (1% SDS, 0.1 M $NaHCO_3$) and proteinase K treated prior to purification of RNA on columns prior to qPCR. 1% of the extract used for immunoprecipitation was purified and used as input control.

Chromatin immunoprecipitation (ChIP) of nucleosomes from C33A2 cells

Chromatin immunoprecipitations were performed using the SimpleChIP® Enzymatic Chromatin IP Kit (Cell Signaling) according to the manufacturer's instructions but with some adjustments. In detail, C33A2 cells were cross-linked in 1% formaldehyde for 10 min at room temperature. The cross-linking reaction was stopped by the addition of glycine to a final concentration of 0.125 M. Cells were lysed in Buffer A and the nuclei were recovered by centrifugation. Nuclei were dissolved in Buffer B and MNase was added to digest the DNA at a final concentration of 0.125 U/µl. Incubation time and amount of enzyme had been previously titrated to achieve mono- and dinucleosomes. Nuclei were resuspended in ChIP buffer, incubated on ice for 10 min and sonicated 10–20 × 15 s using a Diagenode Bioruptor with high setting. Nuclei were observed in a microscope during sonication to ensure that sufficient lysis had occurred. Samples were thereafter subjected to centrifugation and the nuclear extract was recovered. A small aliquot was RNase and proteinase K treated prior to spin column purification to determine the size and concentration of the DNA. For immunoprecipitation, nuclear extract corresponding to 10–15 µg of DNA was diluted in ChIP buffer and antibodies indicated in the figures were added for an overnight end-over-end incubation at 4 °C. Antibodies are listed in Table S2. Immune complexes were precipitated through a two-hour end-over-end incubation at 4 °C with Protein G Magnetic Beads. Beads were washed twice with ChIP buffer, twice with ChIP buffer supplemented with 500 mM NaCl and finally twice with ChIP buffer supplemented with 250 mM LiCl. Each wash was incubated end-over-end for 5 min at 4 °C. Samples were eluted from the beads with elution buffer (1% SDS, 0.1 M $NaHCO_3$) and treated with proteinase K prior to purification of the DNA on spin columns followed by DNA qPCR. 2% of the extract used for immunoprecipitation was purified and used as input control.

Chromatin immunoprecipitation (ChIP) of nucleosomes from HPV16 immortalized 3310 cells

Non-cross linked 3310 cells were lysed in 50 mM Hepes, pH 7.9, 140 mM NaCl, 1 mM EDTA, 0.5% NP-40, 0.25% Triton X-100, 2.5% glycerol and protease inhibitors for 1 h on ice. The intact nuclei were recovered by centrifugation at 14,000 rpm for 1 min. The nuclei were dissolved in 20 mM Tris pH 8.2, 150 mM NaCl, 2 mM EDTA, 0.1% SDS, 1% Triton X-100, protease inhibitors, incubated for 15 min on ice followed by sonication for 10 min (20 × 30 s) using a Diagenode Bioruptor with high setting to disrupt the nuclei and shear the DNA. The DNA fragments were between 200 and 1000 bp. The nuclear extracts were recovered by centrifugation at 14,000 rpm for 10 min. A small aliquot was RNase and proteinase K treated prior to purification of DNA on spin columns to determine the size and concentration of the DNA. For immunoprecipitation, nuclear extracts corresponding to 5 µg of DNA were diluted in ChIP buffer and antibodies were added for overnight end-over-end incubations at 4 °C. Antibodies are listed in Table S2. Immune complexes were precipitated by a 2 h end-over-end incubation at 4 °C with Protein G Magnetic Beads. Beads were washed twice with ChIP buffer, twice with ChIP buffer supplemented with 500 mM NaCl and finally twice with ChIP buffer supplemented with 250 mM LiCl. Each wash was

incubated end-over-end for 5 min at 4 °C. Samples were eluted from the beads with elution buffer (1% SDS, 0.1 M $NaHCO_3$), proteinase K treated and subjected to DNA purification on spin columns prior to qPCR. 2% of the extract used for immunoprecipitation was purified and used as input control.

Acknowledgments

We are grateful to all members of Stefan Schwartz's group for reagents and discussion.

The work was supported by the Swedish Research Council-Medicine [Grant no. 2012-1933], the Swedish Cancer Society [Grant no. CAN 2012/542], by the Gunnar Nilsson Cancer Research Trust Fund, by Hedda and John Forssmans Foundation through the Royal Physiographic Society in Lund and by The Crafoord Foundation [Grant no. 20131005].

Appendix A. Supporting information

Supplementary data associated with this article can be found in the online version at http://dx.doi.org/10.1016/j.virol.2015.02.053.

References

Acuna, L.I.G., Fiszbein, A., Alló, M., Schor, I.E., Kornblihtt, A.R., 2013. Connections between chromatin signatures and splicing. WIREs RNA 4, 77–91.
Andersson, R., Enroth, S., Rada-Iglesias, A., Wadelius, C., Komorowski, J., 2009. Nucleosomes are well positioned in exons and carry characteristic histone modifications. Genome Res. 19, 1732–1741.
Arts, J., King, P., Marien, A., Floren, W., Belien, A., et al., 2009. JNJ-26481585, a novel second-generation oral histone deacetylase inhibitor, shows broad-spectrum preclinical antitumoral activity. Clin. Cancer Res. 15, 6841–6851.
Atadja, P., 2009. Development of the pan-DAC inhibitor panobinostat (LBH589): successes and challenges. Cancer Lett. 280, 233–241.
Baker, C., Calef, C., 1997. Maps of papillomavirus mRNA transcriptsIn: Billakanti, S. R., Calef, C.E., Farmer, A.D., Halpern, A.L., Myers, G.L. (Eds.), Human papillomaviruses: a compilation and analysis of nucleic acid and amino acid sequences. Theoretical Biology and Biophysics, Los Alamos National Laboratory, Los Almos.
Barski, A., Cuddapah, S., Cui, K., Roh, T.-Y., Schones, D.E., et al., 2007. High-resolution profiling of histone methylations in the human genome. Cell 129, 823–837.
Bernard, H.U., 2013. Regulatory elements in the viral genome. Virology 445, 197–204.
Bodily, J., Laimins, L.A., 2011. Persistence of human papillomavirus infection: keys to malignant progression. Trends Microbiol. 19, 33–39.
Bosch, F.X., Lorincz, A., Munoz, N., Meijer, C.J., 2002. The causal relation between human papillomavirus and cervical cancer. J. Clin. Pathol. 55, 244–265.
Bouvard, V., Baan, R., Straif, K., Grosse, Y., Secretan, B., et al., 2009. A review of human carcinogens—Part B: biological agents. Lancet Oncol. 10, 321–322.
Braunschweig, U., Gueroussov, S., Plocik, A.M., Gravely, B.R., Blencowe, B.J., 2013. Dynamic integration of splicing witihn gene regulatory pathways. Cell 152, 1252–1269.
Brown, S.J., Stoilov, P., Xing, Y., 2012. Chromatin and epigenetic regulation of pre-mRNA processing. Hum. Mol. Genet. 21, R90–R96.
Cartegni, L., Chew, S.L., Krainer, A.R., 2002. Listening to silence and understanding nonsense: exonic mutations that affect splicing. Nat. Rev. Genet. 3, 285–298.
Chow, L.T., Broker, T.R., Steinberg, B.M., 2010. The natural history of human papillomavirus infections of the mucosal epithelia. APMIS, 118; , pp. 422–449.
Collier, B., Goobar-Larsson, L., Sokolowski, M., Schwartz, S., 1998. Translational inhibition in vitro of human papillomavirus type 16 L2 mRNA mediated through interaction with heterogenous ribonucleoprotein K and poly(rC)-binding proteins 1 and 2. J. Biol. Chem. 273, 22648–22656.
Doorbar, J., 2005. The papillomavirus life cycle. J. Clin. Virol. 32 (Suppl. 1), S7–S15.
Finzer, P., Kuntzen, C., Soto, U., zur Hausen, H., Rösl, F., 2001. Inhibitor of histone deacetylase arrest cell cycle and induce apoptosis in cervical carcinoma cells circumventing human papillomavirus oncogene expression. Oncogene 20, 4768–4776.
Fraga, M.F., Ballestar, E., Villar-Garea, A., Boix-Chornet, M., Espada, J., et al., 2005. Loss of acetylation at Lys16 and trimethylation at Lys20 of histone H4 is a common hallmark of human cancer. Nat. Genet. 37, 391–400.
Ghosh, S.K., Perrine, S.P., Williams, R.M., Faller, D.V., 2012. Histone acetylase inhibitors are potent inducers of gene expression in latent EBV and sensitize lymphoma cells to nucleoside antiviral agents. Blood 119, 1008–1017.
Graham, S.V., 2008. Papillomavirus 3' UTR regulatory elements. Front. Biosci. 13, 5646–5663.
zur Hausen, H., 2002. Papillomaviruses and cancer: from basic studies to clinical application. Nat. Rev. Cancer 2, 342–350.
Howley, P.M., Lowy, D.R., 2006. Papillomaviridae. In: Knipe, D.M., Howley, P.M. (Eds.), Virology, 5th ed Lippincott/The Williams & Wilkins Co, Philadelphia, PA, pp. 2299–2354.
Iannone, C., Valcárcel, J., 2013. Chromatin's thread to alternative splicing regulation. Chromosoma 122, 465–474.
Jeon, S., Lambert, P.F., 1995. Integration of human papillomavirus type 16 DNA into the human genome leads to increased stability of E6 and E7 mRNAs: implications for cervical carcinogenesis. Proc. Natl. Acad. Sci. USA 92, 1654–1658.
Jia, R., Zheng, Z.M., 2009. Regulation of bovine papillomavirus type 1 gene expression by RNA processing. Front. Biosci. 14, 1270–1282.
Jia, R., Liu, X., Tao, M., Kruhlak, M., Guo, M., et al., 2009. Control of the papillomavirus early-to-late switch by differentially expressed SRp20. J. Virol. 83, 167–180.
Jia, R., Li, C., McCoy, J.P., Deng, C.X., Zheng, Z.M., 2010. SRp20 is a proto-oncogene critical for cell proliferation and tumor induction and maintenance. Int. J. Biol. Sci. 6, 806–826.
Johannsen, E., Lambert, P.F., 2013. Epigenetics of human papillomaviruses. Virology 445, 205–212.
Johansson, C., Schwartz, S., 2013. Regulation of human papillomavirus gene expression by splicing and polyadenylation. Nat. Rev. Microbiol. 11, 239–251.
Johansson, C., Somberg, M., Li, X., Backström Winquist, E., Fay, J., et al., 2012. HPV-16 E2 contributes to induction of HPV-16 late gene expression by inhibiting early polyadenylationEMBO J. 13, 3212–3227.
Li, X., Johansson, C., Glahder, J., Mossberg, A., Schwartz, S., 2013. Suppression of HPV-16 late L1 5′-splice site SD3632 by binding of hnRNP D proteins and hnRNP A2/B1 to upstream AUAGUA RNA motifs. Nucleic Acids Res. 22, 10488–10508.
Li, X., Johansson, C., Cardoso-Palacios, C., Mossberg, A., Dhanjal, S., et al., 2013. Eight nucleotide substitutions inhibit splicing to HPV-16 3′-splice site SA3358 and reduce the efficiency by which HPV-16 increases the life span of primary human keratinocytes. PLoS One 8, e72776.
Longworth, M.S., Laimins, L.A., 2004. The binding of histone deacetylases and the integrity of zinc finger-like motifs of the E7 protein are essential for the life cycle of human papillomavirus type 31. J. Virol. 78, 3533–3541.
Luco, R.F., Misteli, T., 2011. More than a splicing code: integrating the role of RNA, chromatin and non-coding RNA in alternative splicing regulation. Curr. Opin. Genet. Dev. 21, 366–372.
Luco, R.F., Pan, Q., Tominaga, K., Blencowe, B.J., Pereira-Smith, O.M., et al., 2010. Regulation of alternative splicing by histone modifications. Science 327, 996–1000.
Martinez-Redondo, M., Vaquero, A., 2013. The diversity of histone versus non-histone sirtuin substrates. Genes Cancer 4, 148–163.
Matalon, S., Rasmussen, T.A., Dinarello, C.A., 2011. Histone deacetylase inhibitors for purging HIV-1 from the latent reservoir. Mol. Med. 17, 466–472.
McBride, A.A., 2013. The papillomavirus E2 proteins. Virology 445, 57–79.
McBride, A.A., Sakakibara, N., Stepp, W.H., Jang, M.K., 2012. Hitchhiking on host chromatin: how papillomaviruses persist. Biochim. Biophys. Acta 1819, 820–825.
Meyers, C., Frattini, M.G., Hudson, J.B., Laimins, L.A., 1992. Biosynthesis of human papillomavirus from a continuous cell line upon epithelial differentiation. Science 257, 971–973.
Oberg, D., Fay, J., Lambkin, H., Schwartz, S., 2005. A downstream polyadenylation element in human papillomavirus type 16 encodes multiple GGG-motifs and interacts with hnRNP H. J. Virol. 79, 9254–9269.
Orru, B., Cunniffe, C., Ryan, F., Schwartz, S., 2012. Development and validation of a novel reporter assay for human papillomavirus type 16 late gene expression. J. Virol. Methods 183, 106–116.
Pradeepa, M.M., Sutherland, H.G., Ule, J., Grimes, G.R., Bickmore, W.A., 2012. Psip1/Ledgf p52 binds methylated histone H3K36 and splicing factors and contributes to the regulation of alternative splicing. PLOS Genet. 8, e1002717.
Qian, C., Lai, C.-J., Bao, R., Wang, D.-G., Wang, J., et al., 2012. Cancer network disruption by a single molecule inhibitor targeting both histone deacetylase activity and phosphatidylinol 3-kinase signaling. Clin. Cancer Res. 18, 4104–4113.
Rosenberger, S., De-Castro Arce, J., Langbein, L., Steenbergen, R.D.M., Rösl, F., 2010. Alternative splicing of human papillomavirus type-16 E6/E6∗ early mRNA is coupled to EGF signaling via Erk1/2 activation. Proc. Natl. Acad. Sci. USA 107, 7006–7011.
Rush, M., Zhao, X., Schwartz, S., 2005. A splicing enhancer in the E4 coding region of human papillomavirus type 16 is required for early mRNA splicing and polyadenylation as well as inhibition of premature late gene expression. J. Virol. 79, 12002–12015.
Saint-Andre, V., Batsche, E., Rachez, C., Muchardt, C., 2011. Histone H3 lysine 3 trimethylation and HP1gamma favor inclusion of alternative exons. Nat. Struct. Mol. Biol. 18, 337–344.
Schor, I.E., Rascovan, N., Pelish, F., Alló, M., Kornblihtt, A.R., 2009. Neuronal cell depolarization induces intragenic chromatin modifications affecting NCAM alternative splicing. Proc. Natl. Acad. Sci. USA 106, 4325–4330.
Schwartz, S., 2013. Papillomavirus transcripts and posttranscriptional regulation. Virology 445, 187–196.
Schwartz, S., Ast, G., 2010. Chromatin density and splicing destiny: on the cross-talk between chromatn structure and splicing. EMBO J. 29, 1629–1636.
Somberg, M., Schwartz, S., 2010. Multiple ASF/SF2 sites in the HPV-16 E4-coding region promote splicing to the most commonly used 3′-splice site on the HPV-16 genome. J. Virol. 84, 8219–8230.
Somberg, M., Li, X., Johansson, C., Orru, B., Chang, R., et al., 2011. SRp30c activates human papillomavirus type 16 L1 mRNA expression via a bimodal mechanism. J. Gen. Virol. 92, 2411–2421.

Spies, N., Nielsen, C.B., Padgett, R.A., Burge, C.B., 2009. Biased chromatin signatures around polyadenylation sites and exons. Mol. Cell 36, 245–254.
Steenbergen, R.D.M., Snijders, P.J., Heideman, D.A.M., Meijer, C.J., 2014. Clinical implications of (epi)genetic changes in HPV-induced cervical precancerous lesion. Nat. Rev. Cancer 14, 395–405.
Szalmás, A., Kónya, J., 2009. Epigenetic alterations in cervical carcinogenesis. Semin. Cancer Biol. 19, 144–152.
Thierry, F., 2009. Transcriptional regulation of the papillomavirus oncogenes by cellular and viral transcription factors in cervical carcinoma. Virology 384, 375–379.
Tolstorukov, M.Y., Goldman, J.A., Gilbert, C., Ogryzko, V., Kingston, R.E., et al., 2012. Histone variant H2A.Bbd is associated with active transcription and mRNA processing in human cells. Mol. Cell 47, 596–607.
Vermeulen, M., Eberl, H.C., Matarese, F., Marks, H., Denissov, S., et al., 2010. Quantitative interaction proteomics and genome-wide profiling of epigenetic histone marks and their readers. Cell 142, 967–980.
Wagner, B.J., Carpenter, P.B., 2012. Understanding the language of Lys36 methylation at histone H3. Nat. Rev. Mol. Cell Biol. 13, 115–126.
Walboomers, J.M., Jacobs, M.V., Manos, M.M., Bosch, F.X., Kummer, J.A., et al., 1999. Human papillomavirus is a necessary cause of invasive cervical cancer worldwide. J. Pathol. 189, 12–19.
Wang, Z., Zang, C., Rosenfeld, M.G., Schones, D.E., Barski, A., et al., 2008. Combinatorial patterns of histone acetylations and methylations in the human genome. Nat. Genet. 40, 897–903.
Yuan, H., Myers, S., Wang, J., Zhou, D., Woo, J.A., et al., 2012. Use of reprogrammed cells to identify therapy for respiratory papillomatosis. N. Engl. J. Med. 367, 1220–1227.
Zhao, X., Schwartz, S., 2008. Inhibition of HPV-16 L1 expression from L1 cDNAs correlates with the presence of hnRNP A1 binding sites in the L1 coding region. Virus Genes 36, 45–53.
Zhao, X., Rush, M., Schwartz, S., 2004. Identification of an hnRNP A1 dependent splicing silencer in the HPV-16 L1 coding region that prevents premature expression of the late L1 gene. J. Virol. 78, 10888–10905.
Zhao, X., Öberg, D., Rush, M., Fay, J., Lambkin, H., et al., 2005. A 57 nucleotide upstream early polyadenylation element in human papillomavirus type 16 interacts with hFip1, CstF-64, hnRNP C1/C2 and PTB. J. Virol. 79, 4270–4288.
Zhao, X., Fay, J., Lambkin, H., Schwartz, S., 2007. Identification of a 17-nucleotide splicing enhancer in HPV-16 L1 that counteracts the effect of multiple hnRNP A1-binding splicing silencers. Virology 369, 351–363.
Zhou, H.-L., Hinman, M.N., Barron, V.A., Geng, C., Zhou, G., et al., 2011. Hu proteins regulate alternative splicing by inducing histone hyperacetylation in an RNA-dependent manner. Proc. Natl. Acad. Sci. USA 108, E627–E635.